J. H. Scofield and D. M. Fleetwood, *IEEE Transactions on Nuclear Science* **NS-38**, 1567-77 (December 1991).

PHYSICAL BASIS FOR NONDESTRUCTIVE TESTS OF MOS RADIATION HARDNESS*

John H. Scofield
Department of Physics, Oberlin College
Oberlin, OH 44074

and

D.M. Fleetwood
Sandia National Laboratories
Albuquerque, NM 87185-5800

Abstract

We have found that the 1/f noise and channel resistance of unirradiated nMOS transistors from a single lot with various gate-oxide splits closely correlate with the oxide-trap and interface trap charge, respectively, following irradiation. The 1/f noise is explained by a trapping model, while the variations in channel resistance are explained by scattering from interface-trap precursor defects. It appears that both noise and channel mobility measurements may be useful in defining nondestructive hardness assurance test methods for devices fabricated from a single technology. It may be difficult to use either for making cross-technology comparisons. Finally, during the course of this study it was found that process techniques that improve the radiation hardness of MOS devices at room temperature can greatly reduce the 1/f noise of MOS devices at cryogenic temperatures.*

1. Introduction

Traditional methods to determine the radiation hardness of MOS structures require destructive testing. MOS devices are fielded in radiation environments on the basis of test results on a small sample of devices that are expected to show hardness levels typical of the larger (untested) population. The inability to directly measure the hardness of a fielded device can increase the cost of a radiation-hardened system and decrease one's level of confidence that the system will perform as intended in the use environment. It is therefore useful to consider whether nondestructive methods can be defined to characterize the hardness of MOS structures prior to their system use. In this abstract, we consider the physical basis for nondestructive methods to predict MOS oxide- and interface-trap charge buildup in a radiation environment.

In previous work, a strong correlation was observed between the *preirradiation* 1/f-noise of MOS transistors, measured at room temperature, and their *postirradiation* oxide-trap charge [1,2]. Here we expand the work by reporting the results of measurements on two additional kinds of nMOS transistors. In addition, noise measurements have been extended to include temperatures in the range 80 - 300K. These results are used to expand upon a trapping model of the noise. The evidence suggests that the noise and the oxide-trap charge are both influenced by the preirradiation density of oxygen vacancies in the SiO_2 [2].

We also demonstrate a striking correlation between the *preirradiation* channel resistance of MOS transistors and their *postirradiation* interface-trap charge [3]. We have developed a model that relates the preirradiation 1/f-noise to the net radiation-induced oxide charge-trapping efficiency [2], and a model that relates the preirradiation channel mobility to radiation-induced interface trap generation efficiency [3]. We conclude that, even before a device is irradiated, carrier-defect interactions evidently reveal a great deal of information about the radiation hardness of MOS devices. Implications for hardness assurance testing are discussed.

2. Experimental Details

2.1 Samples

DC conductance, excess noise, and radiation hardness measurements were performed on nMOS transistors from a variety of wafers. Except for the growth and annealing of their gate oxides, seven of the wafers (Lot G1916A) were processed identically using Sandia's old baseline process. Devices from these wafers have dimensions L = (3.45±0.10) μm and W = (16.0±0.5) μm. The processing of these wafers has been described elsewhere [1,2]. Measurements have also been performed on devices from two additional wafers, one from AT&T's 1-μm radiation hardened technology (Lot 11370, Wafer 50) [4] and the other from Sandia's 3-μm "mod B" radiation tolerant technology (Lot DE152D, Wafer 22) [5]. Devices from this latter wafer have identical dimensions to those listed above and an oxide thickness of 45 nm. AT&T devices had an oxide thickness of 18 nm, with L = 5 μm and W = 30 μm.

2.2 DC Conductance

DC conductance measurements were performed on all devices with sources and substrates grounded at two

* This work was supported by the U.S. Department of Energy and by the Defense Nuclear Agency.

temperatures, 80 K and 300 K. Devices were operated in their linear regimes, i.e., for sufficiently small drain currents (I_d) such that their drain voltages (V_d) and drain currents satisfied

$$I_d = gV_d. \quad (1)$$

As expected the dc-channel conductance (g) was found to increase linearly with the gate voltage (V_g), that is

$$g = \beta(V_g - V_T), \quad (2)$$

where V_T is the threshold voltage [6]. We refer to β^{-1} as the channel "resistance parameter" as it is essentially equal to the channel resistance for an "effective" gate voltage $V_g - V_T = 1V$. Plots of channel conductance versus gate voltage were used to extract V_T and β^{-1} for each device at room temperature. The carrier mobility μ and β^{-1} are related via

$$\beta = C_{ox} \left(\frac{W}{L}\right) \mu, \quad (3)$$

where $C_{ox} = \varepsilon_{ox}/t_{ox}$ is the oxide capacitance per unit area and ε_{ox} and t_{ox} are the oxide permittivity and thickness respectively. The results of conductance measurements are shown in Table I. Also shown, for later comparison, are the radiation-induced threshold shifts due to interface-trap charge (ΔV_{it}) and the interface-trapping efficiencies (f_{it}). These quantities are discussed below. Measurement details may be found elsewhere [3].

2.3 Excess Noise

Noise measurements at 80-300 K were performed on devices operated in their linear regimes with their sources and substrates grounded. Devices were biased with constant I_d and V_g, and fluctuations $\delta V_d(t)$ in the drain voltage were characterized for frequencies between 5 Hz and 50 kHz. Details of the measurements are described elsewhere [1].

The room-temperature excess drain-voltage noise spectrum S_V (i.e., measured noise minus background noise) of each device was consistent with

$$S_V(f, I_d, V_g) = \frac{K}{f^\gamma} \frac{V_d^2}{(V_g - V_T)^2}, \quad (4)$$

where the device-dependent noise level K and frequency exponent γ were chosen to fit the data. γ was found to be very close to unity for all of the devices, i.e., "1/f noise."[1] The room-temperature noise levels, oxide thicknesses, and channel geometries are summarized in Table II. Also listed in Table II, for later comparison, are the radiation-induced threshold shifts due to oxide-trap charge (ΔV_{ot}) and the oxide-trapping efficiencies (f_{ot}). These quantities are discussed below.

2.4 Radiation Hardness

To characterize their radiation response, devices were exposed to 100 krad(SiO_2) in a Co-60 gamma cell at a dose rate of 1 Mrad/h. An oxide electric field of 3 MV/cm was maintained during irradiation. Threshold shifts due to irradiation (ΔV_T) were separated into components ΔV_{ot} and ΔV_{it} due to oxide- and interface-trap charge using the method of Winokur and McWhorter [7]. Threshold shifts due to interface-trap charge are summarized in Table I and those due to oxide-trap charge are shown in Table II. The nine wafers include a wide range of radiation responses, with ΔV_{it} ranging from 0.01 to 0.56 V (nearly two orders of magnitude) and $|\Delta V_{ot}|$ ranging from 0.02 to 3.53 V (more than two orders of magnitude). The details of the radiation response measurements may be found elsewhere [1].

The radiation-induced threshold shifts depend on radiation dose (D), oxide thickness, and bias. These dependencies are removed by defining dimensionless quantities, f_{ot} and f_{it}, that characterize the inherent "trappiness" of the oxides. The oxide charge-trapping efficiency, f_{ot}, is the ratio of the number of trapped holes to the number of electron-hole (e-h) pairs created; f_{ot} and ΔV_{ot} are related through

$$-\Delta V_{ot} = \frac{e\, \kappa_g\, f_y\, D\, t_{ox}^2}{\varepsilon_{ox}}\, f_{ot}, \quad (5)$$

where κ_g is the number of electron-hole (e-h) pairs produced per unit dose and f_y is the probability that an e-h pair escapes recombination.[2] The interface-trapping efficiency, f_{it}, is defined similarly in terms of ΔV_{it} [2,3]. Values of f_{it} and f_{ot} for the various devices are summarized in Tables I and II respectively.

3. Excess Noise and Oxide-Trap Charge

3.1 Experimental

It has previously been reported that the room-temperature 1/f noise levels of unirradiated devices from the seven G1916A wafers correlate strongly with their net radiation-induced oxide-trap charge [1,2]. Here we include data from the two additional wafers. Since one of these devices has a different geometry from the rest, we must first account for the different gate area. Noise measurements from devices of different gate area on the

---

[1] For very small devices (e.g., 1μm x 1 μm) on the AT&T chips, noise spectra differed significantly from an inverse frequency dependence. This behavior has been observed before in small devices and is to be expected.

[2] For the irradiation conditions and devices employed in this study κ_g = (8.1±0.9) x 10^{12} cm^{-3} $rad^{-1}(SiO_2)$, f_y = (0.90±0.05), and D = 100 krad(SiO_2). Equation (4) is valid only for doses low enough that ΔV_{ot} is approximately linear with D (D< 1 Mrad(SiO_2) for these devices).

same chip show that the noise level K is inversely proportional to gate area, A = LW [8]. Accordingly, Figure 1 shows a plot of KA versus $-\Delta V_{ot}$ for devices from all nine wafers. The open symbols are data from the seven G1916A wafers that have been previously reported [1,2]; the solid symbols represent new data. The triangles are for (nominally) 3 μm x 16 μm devices while the square is for the 5 μm x 30 μm AT&T device. Figure 1 demonstrates a clear correlation between preirradiation 1/f noise and radiation-induced oxide-trap charge for the G1916A and AT&T devices. An analogous graph of KA versus ΔV_{it} shows that no such correlation exists between the 1/f noise of unirradiated devices and their radiation-induced interface-trap charge.

Wafer I.D.	t_{ox} (nm)	V_T (V)	β^{-1} (kΩV)	μ (cm^2/V-s)	ΔV_{it} (mV)	f_{it}
G1916A - 21	32	0.61	2.77±11%	800±12%	120±10	0.034±0.005
G1916A - 22	32	0.70	3.06±10%	768±11%	150±10	0.043±0.005
G1916A - 09	32	0.89	3.50± 4%	586± 6%	240±40	0.068±0.009
G1916A - 10	32	0.94	3.78± 2%	570± 5%	310±30	0.088±0.01
G1916A - 32	48	1.06	4.37± 7%	667± 8%	320±20	0.040±0.005
G1916A - 33	48	1.38	5.12± 1%	578± 5%	560±20	0.071±0.009
G1916A - 44	60	1.47	5.07± 2%	752± 5%	560±30	0.045±0.005
DE152D-22	45	1.27	3.26± 5%	860± 8%	70±10	0.010±0.002
11370-50	18	1.09	14.0± 5%	-------	15±5	0.014±0.004

Table I. Summary of room-temperature resistance data for devices along with radiation-induced interface-trapped charge data. Shown are oxide thickness (t_{ox}), preirradiation threshold voltage (V_T), resistance parameter (β^{-1}), carrier mobility (μ), threshold shift due to interface-trapped charge following irradiation to 100 krad(SiO_2) in a Co-60 cell, and interface-trapping efficiency (f_{it}). Values of μ cannot be inferred from β^{-1} for 11370-50 because of the source resistance associated with its lightly-doped drain.

Wafer I.D.	t_{ox} (nm)	L x W $(\mu m)^2$	K $(\mu V)^2$	$-\Delta V_{ot}$ (V)	f_{ot}
G1916A - 21	32	3.5 x 16.	70± 20	0.20±0.01	0.057±0.008
G1916A - 22	32	3.5 x 16.	70± 20	0.19±0.01	0.054±0.008
G1916A - 09	32	3.5 x 16.	700±100	1.69±0.09	0.48 ±0.06
G1916A - 10	32	3.5 x 16.	530±110	1.88±0.10	0.54 ±0.07
G1916A - 32	48	3.5 x 16.	180± 30	0.32±0.02	0.066±0.009
G1916A - 33	48	3.5 x 16.	1300±250	3.53±0.13	0.45 ±0.06
G1916A - 44	60	3.5 x 16.	220± 80	0.76±0.02	0.062±0.008
DE152D-22	45	3.5 x 16.	300± 50	0.17±0.02	0.025±0.003
11370-50	18	5.0 x 30.	3± 1	0.02±0.01	0.020±0.003

Table II. Summary of room-temperature noise data for unirradiated devices along with radiation-induced oxide-trapped charge data. Shown are oxide thickness (t_{ox}), gate length (L) and width (W), noise level K, threshold shift due to oxide-trapped charge following irradiation to 100 krad(SiO_2) in a Co-60 cell, and net oxide charge-trapping efficiency (f_{ot}).

Note that one of the new data points (AT&T) agrees well with our previous data [1,2] while the second point (DE152D) does not. We now discuss why the response of DE152D may differ from that of the other wafers. The measured drain-voltage noise represents a weighted average of noise properties, both along the channel and from the drain and source contacts. Contacts can be notorious sources of 1/f noise, and, in these inherently two-probe measurements, there is no way to distinguish contact noise from channel noise. Devices on the DE152D wafer differ from the other devices in that the technology used to fabricate their contacts yields higher resistance contacts. These contacts may contribute significant 1/f noise of their own.

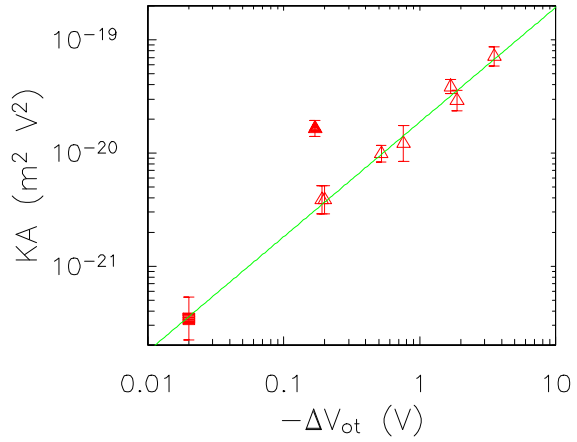

Figure 1. Gate-area-scaled noise level (KA) of unirradiated devices versus the threshold shift (ΔV_{ot}) due to net oxide-trapped charge following irradiation of similar devices to a total dose of 100 krad(SiO_2). The line represents a least-squares fit to all but one of the points.

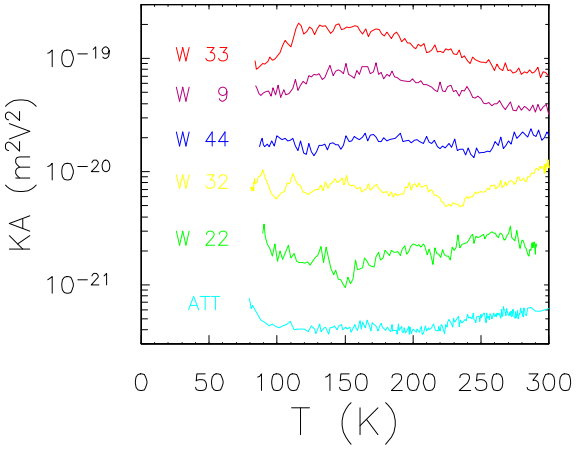

Figure 2. Gate-area-scaled noise level KA of selected unirradiated devices versus temperature.

Also, thermally-stimulated current measurements on capacitors processed similarly to DE152D suggest that there may be a significantly higher amount of trapped holes than indicated by ΔV_{ot}, but that they are compensated by trapped electrons [9]. Additional experiments are ongoing to determine whether these or other factors increase the noise of DE152D above other wafers. The implication of this result for hardness assurance testing will be addressed below in Section 5.

Figure 2 shows the temperature dependence of the noise levels of selected devices. Data not shown behave similarly.[3] Note that, while the noise level of a particular device does vary with temperature, the relative ordering of the noise levels of the various devices does not depend on temperature, i.e., the noisiest devices at 300 K are the noisiest at 80 K. As a consequence, the correlation shown in Figure 1 between K(300K) and ΔV_{ot} would be equally valid for K measured throughout the entire temperature range. We conclude from Figure 2 that methods to harden MOS oxides at room temperature can significantly reduce their noise at cryogenic temperatures. This is a key point for cryogenic MOS applications.

We should also mention that the correlation between K and oxide-trap charge for similar nMOS devices has been studied through irradiation and annealing [10]. Experiments show that the 1/f noise level (K), ΔV_{ot}, and ΔV_{it} all increase linearly with radiation dose. Upon annealing, however, both ΔV_{ot} and K decrease (proportionally) while ΔV_{it} does not. We conclude that, both before and after irradiation, 1/f noise is very sensitive to traps in the MOS oxide.

3.2 Trapping Model for the Noise

A variety of models have been proposed to explain 1/f noise in MOSFETs [8,11-18]. After much controversy, it is now widely accepted that the noise of MOSFETs is associated with capture and emission of charge carriers from traps in the oxide, very near to the Si/SiO_2 interface [14]. Fluctuations in oxide-trap charge couple to the channel, both directly through a compensating change in the inversion layer charge density, and indirectly through fluctuations in scattering associated with the fluctuating trapped charge. The former mechanism is referred to as "number" fluctuations while the latter is termed "mobility" fluctuations.[4] Data from narrow-channel MOSFETs confirm that both effects can be important [19]. In general, noise studies on n-channel MOSFETs tend to agree with predictions that neglect the mobility fluctuation mechanism while studies on p-channel MOSFETs do not [14]. Our own data confirm this behavior [20]. It has been suggested that the noise of p-channel devices involve both number and mobility fluctuations [14,18].

In this section, we expand upon a simple trapping model of the noise introduced earlier [1]. Here, we draw on the work of a variety of authors that treat generally the same model [8,11-18,21,22].

[3] The one exception to this is the noise of the DE152D devices for which K(T) increases with decreasing T by an order-of-magnitude between 120K and 80K. We do not know if the anomalous temperature dependence of the noise of these devices is related to their anomalously-high room temperature noise level (Figure1) .

[4] Here the phrase "mobility fluctuations" is used to refer to fluctuations associated with any scattering mechanism. Some authors use this term specifically to refer to fluctuations in phonon scattering.

Figure 3 shows a diagram of the energy bands of an nMOS transistor near the Si/SiO_2 interface when the device is operated in strong inversion. Oxide traps are continually emitting and capturing electrons to/from the inversion layer. We assume that this fluctuating trapped charge couples to the channel by causing a fluctuating "effective" gate voltage, i.e. number fluctuations. We neglect fluctuations in scattering associated with these traps, and calculate only the impact of carrier number fluctuations on the noise.[5]

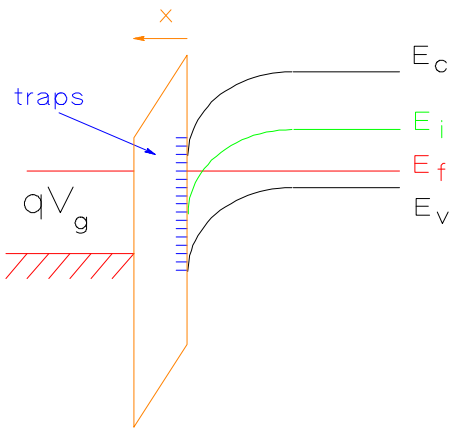

Figure 3. Energy band diagram near the Si/SiO_2 interface of an n-channel MOSFET biased in inversion.

Let $n_{ot}(E,x)\,dx\,dE$ be the number of oxide states per unit area having an energy between E and E+dE and located between a distance x and x+dx (in the oxide) from the Si/SiO_2 interface. The probability that one of these states is occupied (i.e., contains a trapped electron) is given by the fermi factor

$$F(E) = \frac{1}{\exp\left(\frac{E-E_f(T)}{kT}\right)+1}\,, \qquad (6)$$

where $E_f = E_f(T)$ is the fermi level. The mean density (number per unit volume per unit energy) of trapped electrons is given by

$$<n_t(E,x)> = n_{ot}(E,x)\,F(E)\,. \qquad (7)$$

The mean number per unit area, $<N_t>$, of trapped electrons is thus obtained by integrating the above expression over the oxide thickness and bandgap, i.e.

$$<N_t> = \int_{E_v}^{E_c}\int_{0}^{t_{ox}} n_{ot}(E,x)\,F(E)\,dx\,dE\,, \qquad (8)$$

where E_v and E_c are the valence- and conduction-band energies of the SiO_2. The localized oxide states are assumed to communicate with the inversion layer via tunneling. Thus, in thermal equilibrium there will be fluctuations $\delta n_t(E,x)$ about the equilibrium concentration. The mean-square fluctuation (i.e., variance) is given by [23]

$$<\delta n_t^2(E,x)> = \frac{<n_{ot}(E,x)>}{LW}\,F(E)\,[1-F(E)]\,, \qquad (9)$$

and, of course, the variance in the total number of oxide-trapped charges $<\delta N_t^2>$ is obtained by integrating the above over E and x,

$$<\delta N_t^2> = \frac{1}{LW}\int_{E_v}^{E_c}\int_{0}^{t_{ox}} n_{ot}(E,x)\,F(E)\{1-F(E)\}\,dx\,dE. \qquad (10)$$

We now assume that a non-equilibrium concentration $n_t(E,x)$ relaxes to equilibrium exponentially with a time-constant, $\tau = \tau(E,x)$. The autocorrelation function $G_{n_t}(\Delta t)$ of fluctuations $\delta n_t(E,x)$ is then obtained via the fluctuation-dissipation theorem,

$$G_{n_t}(\Delta t) = <\delta n_t^2>\exp(-|\Delta t|/\tau)\,, \qquad (11)$$

where the dependence on E and x is implied but not explicitly written. The corresponding power spectral density, $S_{n_t}(f)$, is obtained using the Wiener-Khintchine theorem as the Fourier transform of the autocorrelation function, namely

$$S_{n_t}(f) = \frac{4\,\tau\,<\delta n_t^2>}{1+(2\pi f\,\tau)^2}\,, \qquad (12)$$

which is the familiar Debye-Lorentzian spectrum. The power spectral density of fluctuations in total number of trapped charges is obtained by substituting Eq. (9) into Eq. (12) and integrating over E and x, that is

[5] Our justification for neglecting mobility fluctuations is that the simple trapping model is in excellent agreement with the data.

$$S_{N_t}(f,T) = \frac{1}{LW}\int_0^{t_{ox}}\int_{E_v}^{E_c} n_{ot}(E,x)\;F(E)\{1-F(E)\}\;\frac{4\tau(E,x)}{1+\{2\pi f\,\tau(E,x)\}^2}\,dE\,dx \qquad (13)$$

where the E- and x-dependencies have been explicitly noted. The trap density $n_{ot}(x,E)$ is assumed to be a slowly-varying function of energy E. In this case, the factor F(1-F) acts like a "delta function" of width kT near the fermi level, so that the energy integral is trivially performed leaving

$$S_{N_t}(f,T) \approx \frac{kT}{LW}\int_0^{t_{ox}} n_{ot}(E_f,x)\,\frac{4\tau(E_f,x)}{1+\{2\pi f\,\tau(E_f,x)\}^2}\,dx, \qquad (14)$$

where k is the Boltzmann constant. Thus, the level of the noise spectrum is determined by the density of traps near the fermi level and the frequency components are determined by their distribution in distance from the Si/SiO_2 interface and the exact nature of the relaxation time.

To make further progress we must assume something about the relaxation times. As is commonly done in the literature, we assume that the mean trapping time is governed by tunneling and is given by

$$\tau(E,x) = \tau_0(E)\,e^{\zeta x}, \qquad (15)$$

where ζ is a tunneling parameter [21]. Furthermore, we assume that $n_t(E_f,x)$ is constant for $0 < x < x_1$, where $x_1 << t_{ox}$, and zero for $x > x_1$. With these assumptions, Eq. (14) reduces to

$$S_{N_t}(f,T) \approx \frac{4\,kT\,n_{ot}(E_f)}{LW}\int_0^{x_1}\frac{\tau_0\,e^{\zeta x}}{1+\{2\pi f\,\tau_0\,e^{\zeta x}\}^2}\,dx, \qquad (16)$$

and, since $d\tau/\zeta = \tau\,dx$, we have

$$S_{N_t}(f,T) \approx \frac{4\,kT\,n_{ot}(E_f)}{LW\,\zeta}\int_{\tau_0}^{\tau_1}\frac{d\tau}{1+(2\pi f\,\tau)^2}, \qquad (17)$$

where $\tau_1 = \tau_0\exp(\zeta x_1)$. This integral is easily performed giving the spectrum as

$$S_{N_t}(f,T) \approx \frac{4\,kT\,n_{ot}(E_f)}{2\pi f\,\zeta\,LW}\{\tan^{-1}(2\pi f\tau_1) - \tan^{-1}(2\pi f\tau_0)\}. \qquad (18)$$

The measured noise spectrum is inversely proportional to frequency for all f. For the measured spectrum to be described by Eq. (18) it must be that the low- and high-frequency cut-offs satisfy: $2\pi f\tau_1 >> 1$ and $2\pi f\tau_0 << 1$. Thus, for all measurement frequencies, the first term in the brackets will be $\pi/2$ and the second term will be zero. With these assumptions Eq. (18) reduces to

$$S_{N_t}(f,T) \approx \frac{kT\,D_t(E_f)}{LW\,\ln(\tau_1/\tau_0)}\,\frac{1}{f}. \qquad (19)$$

where $D_t(E) \equiv \int n_{ot}(E,x)\,dx \approx x_1\,n_{ot}$.[6] Note that the noise yields information about the traps at the fermi level at a distance from the interface that depends on f. The fermi level depends on temperature but does not vary with gate-voltage. Due to band bending, however, the trap energy (relative to the fermi level) does depend on V_{gs}. Thus the traps that give rise to the measured noise depend on f, T, and V_g. If $n_{ot}(E,x)$ is not constant, but varies slowly with distance from the interface then the resulting spectrum retains the form of Eq. (19), but with a frequency exponent that is not exactly unity [22,24].

We also note that these same assumptions about $n_{ot}(x,E)$ may be inserted into Eq. (8) and Eq. (10) to obtain

$$\langle N_t\rangle = \int_{E_v}^{E_c} D_t(E)\,F(E)\,dE, \qquad (20)$$

and $\langle \delta N_t^2\rangle \approx \frac{kT}{LW}\,D_t(E_f)$.

Equation (19) above describes the power spectral density of the fluctuations in the number of trapped electrons as a function of frequency and temperature. This fluctuating trapped charge must be related to the measured quantity, namely, fluctuations in the drain voltage under constant gate-voltage and drain current bias. As the oxide traps communicate with the channel, we assume that there will be fluctuations in the density of trapped charge, $\delta Q_t = -e\delta N_t$. For strong inversion, these fluctuations in trapped charge result in a fluctuation in the effective gate voltage,

$$\delta V_g = \delta Q_t/C_{ox}. \qquad (21)$$

and, with the device operated in the linear regime with fixed drain current, a fluctuation in drain voltage,

$$\delta V_d = (\partial V_d/\partial V_g)\,\delta V_g. \qquad (22)$$

The derivative may be calculated from $V_d = I_d/g$, where $g = g(V_g)$ is given by Eq. (2). Thus, the resulting fluctuation in drain-voltage is simply related to the fluctuating trapped charge density δN_t via[7]

---

6 We note that the dimensions of $D_t(E)$ are number per unit energy per unit area.

7 Since the devices are operated with $V_d << (V_g - V_T)$ we neglect any variation in the carrier density along the channel.

$$\delta V_d = \left(\frac{e}{C_{ox}} \frac{V_d}{(Vg\text{-}V_T)}\right)\delta N_t \,. \qquad (23)$$

Combining this equation with the spectrum $S_{N_t}(f,T)$ we have

$$S_V\,(f,T,V_d,V_g) = \left(\frac{eV_d}{C_{ox}(Vg\text{-}V_T)}\right)^2 S_{N_t}(f,T). \qquad (24)$$

The above expression shows that the measured power spectrum is completely determined by the distribution of traps. Comparing Eqs.(4) and (24) we see that, for $\gamma = 1$, the phenomenological noise level K is given by

$$K\,(T) = \frac{e^2\, kT\, t_{ox}^2\, D_t(E_f)}{LW\, \varepsilon_{ox}^2\, \ell n(\tau_1/\tau_0)}\,. \qquad (25)$$

In addition to the explicit linear dependence on temperature, K also depends on T through $D_t(E_f(T))$. If the trap density is independent of E then K will be proportional to T. If, on the other hand, D_t varies throughout the bandgap, then this will be reflected in the temperature-dependence of the noise magnitude (see Figure 2). Moreover, the frequency-dependence of the noise spectrum will reflect any dependence of n_{ot} on x [22,24]. Note that K may be used to solve for the density of traps at the fermi level, $D_t(E_f)$.

3.3 Relating Noise to ΔV_{ot}

The basic connection between K and ΔV_{ot} has been outlined elsewhere [2]. Here we expand on the previous discussion. In relating the preirradiation 1/f noise to the radiation-induced threshold shift due to oxide-trap charge ΔV_{ot}, the underlying assumption is that both phenomena are related to the same *preirradiation* defect density, $n_{ot}(E,x)$. The noise has already been related to n_{ot}; we now turn to the task of relating ΔV_{ot} to n_{ot}.

While the noise is sensitive only to those defects very close to the interface and near the fermi level, the radiation-induced oxide-trap charge samples all traps irrespective of their position and energy. We assume that f_{ot} is proportional to the integral of $n_{ot}(E,x)$ over E and x, namely

$$f_{ot} = \sigma \int_{E_v}^{E_c} \int_{0}^{t_{ox}} n_{ot}(E,x)\, dx\, dE, \qquad (26)$$

where σ is the capture cross-section and the energy-integral is over the bandgap of the SiO_2.[8] For the noise model we have already assumed an x-distribution for n_{ot}, making the x-integral above trivial.

To make further progress we must assume something about the energy dependence of $n_{ot}(x,E)$. For simplicity we assume that $n_{ot}(x,E)$ is constant in energy throughout the oxide bandgap.[9] With these assumptions, Eq. (26) reduces to

$$f_{ot} = \sigma\, E_g\, D_t\,, \qquad (27)$$

where D_t is as previously defined and E_g is the SiO_2 bandgap (9 eV). Combining Eqs. (5), (25) and (27) we find that K and ΔV_{ot} are related via

$$LW\, K(T) = \frac{kT}{K_g\, f_y\, D\, \sigma\, E_g\, \varepsilon_{ox}}\,(-\Delta V_{ot}). \qquad (28)$$

The above equation predicts the linear relation between KA and ΔV_{ot} of Figure 1. It should be noted, however, that both K and ΔV_{ot} scale with t_{ox}^2 (see Eqs. (5) and (25)), so that some of the correlation of Figure 1 is associated trivially with variation in t_{ox} among the wafers (see Table II). The dependencies of K and ΔV_{ot} on t_{ox} may be removed by considering KA/t_{ox}^2 and f_{ot} respectively. Changing to these quantities Eq. (28) becomes

$$\frac{LW}{t_{ox}^2}\; K(T) = \left(\frac{e^2\, kT}{\sigma\, E_g\, \varepsilon_{ox}^2\, \ell n(\tau_1/\tau_0)}\right) f_{ot}. \qquad (29)$$

The prediction of the above equation is verified by the graph in Figure 4. The nine data points in Figure 4 fall into four clumps corresponding to four different f_{ot} values. As mentioned above, some of the correlation between KA and ΔV_{ot} of Figure 1 was indeed related to their mutual dependencies on t_{ox}. With the t_{ox} variation accounted for, however, Figure 4 shows clear correlation between the preirradiation noise and the oxide-trapping efficiency predicted by the model, with the exception of DE152D noted above.

8 For simplicity we assume σ is independent of energy.

9 The assumption is obviously not true (as indicated by the temperature dependence of K in Figure2), but in the absence of better information it will allow us to get an order-of-magnitude estimate of the total number of traps.

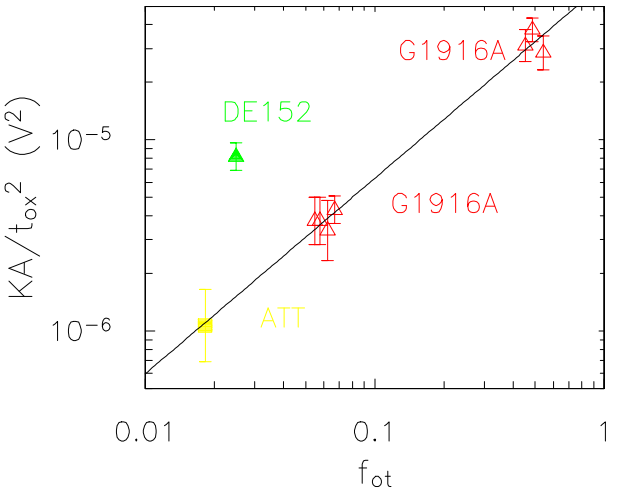

Figure 4. Correlation between preirradiation 1/f noise level and oxide-trapping efficiency with the effects associated with variation in oxide-thickness removed..

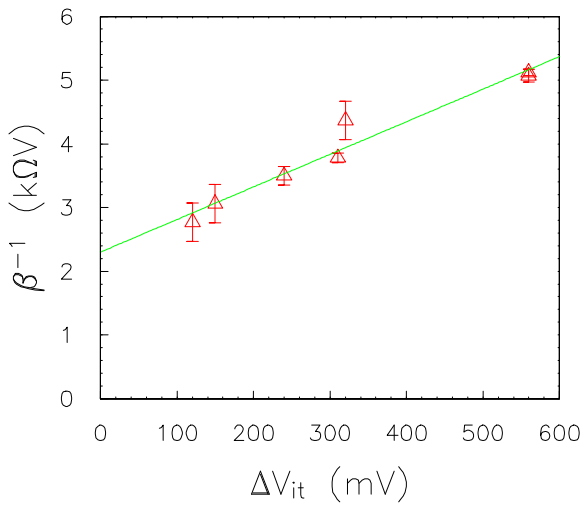

Figure 5. Channel resistance parameter (β^{-1}) of unirradiated devices versus the threshold shift of similar devices due to interface-trapped charge following irradiation to a total dose of 100 krad(SiO_2).

4. Mobility and Interface-Trap Charge

4.1 Correlation Between Preirradiation Resistance and Interface-Trap Charge

While the 1/f noise of unirradiated devices yields information about the oxide-trap charge of irradiated devices, it does not yield information about radiation-induced interface-trap charge. We have found, however, that the channel resistance parameters (β^{-1}) of unirradiated devices correlate with interface-trap charge in irradiated devices from lot G1916A. As these results have been described elsewhere [3] we will merely summarize the results here for completeness. The implications for hardness assurance testing (not previously discussed) will also be addressed below.

Figure 5 shows a plot of the channel resistance parameters of unirradiated devices from lot G1916A versus the radiation-induced threshold shift due to interface-trap charge. As we are concerned with small differences in channel resistance, we have only included data for devices from G1916A wafers which received different oxide processing, but all other processing was the same. The figure shows a clear correlation between β^{-1} and ΔV_{it} for these devices, suggesting that variations in the scattering in unirradiated devices are related to variations in their radiation response due to interface-trap charge. We note here that a similar plot of β^{-1} versus ΔV_{ot} does not show such a strong correlation.

Both β^{-1} and ΔV_{it} increase with t_{ox} so that, as was the case for Figure 1, variation in t_{ox} among our samples accounts trivially for some of the correlation shown in Figure 5. Nevertheless, inspection of Table I shows that there are significant differences in β^{-1} among devices with equal t_{ox}. Below we consider a model that explains the thickness-independent portion of the correlation.

4.2 Scattering Model

The dependence of β^{-1} and ΔV_{it} on oxide thickness may be removed by focusing on carrier mobility instead of channel resistance (see Eq.(3)), and on the interface-trapping efficiency, f_{it}, instead of ΔV_{it}. (The interface-trapping efficiency is defined by replacing "ot" with "it" in Eq.(5)). Before irradiation, various scattering mechanisms contribute to the carrier mobility, and hence the channel resistance. Each scattering mechanism has associated with it a component of mobility μ_j. Matthiessen's rule gives the carrier mobility as

$$\mu^{-1} = \sum_j (\mu_j^{-1}). \qquad (30)$$

The room-temperature mobility of relatively defect-free devices is determined by lattice scattering, ionized-impurity scattering, and "surface" scattering. Lattice scattering, ionized-impurity scattering, and many scattering mechanisms associated with the Si/SiO_2 interface are similar for all devices. Scattering mechanisms common to all devices are represented by μ_0. Variation of the *preirradiation* carrier mobilities indicates that at least one surface-scattering mobility component, μ_p, differs among the devices. We assume that μ_p is inversely proportional to the areal density (n_p) of some "unspecified" interface defect present prior to irradiation, i.e., $1/\mu_p = \gamma n_p$, where γ is the

proportionality constant. Thus, the preirradiation mobility may be written as

$$\frac{1}{\mu} = \frac{1}{\mu_o} + \gamma n_p \, . \tag{31}$$

Prior to irradiation, we assume there exists a density n_{pit} of defects that are "precursors" to the radiation-induced interface trap. (All densities here are per unit gate area.) It is tempting to simply suggest that the postirradiation ΔV_{it} is proportional to n_{pit}. However, just as we normalized out the effects of device geometry by expressing the channel resistance variations in terms of μ, so we must normalize out the effects of device geometry and radiation dose on ΔV_{it}. This is easily accomplished by considering the interface-trapping efficiency, f_{it}, which does not depend on t_{ox}. It is assumed that f_{it} is proportional to the precursor defect density, i.e. $f_{it} = \sigma_p n_{pit}$, where σ_p is a proportionality constant.

Finally, we assume that the defects responsible for the variation in preirradiation mobility are related to those that give rise to the radiation-induced interface traps. Specifically, we assume that $n_p = \lambda n_{pit}$.[10] This leads to the final expression that relates the preirradiation mobility μ to the interface-trap buildup efficiency f_{it},

$$\frac{1}{\mu} = \frac{1}{\mu_o}(1 + \alpha f_{it}) \tag{32}$$

where $\alpha = \lambda\gamma\mu_o/\sigma_p$ is a combination of the various proportionality constants. Figure 6, a plot of $1/\mu$ versus f_{it}, verifies the linear dependence predicted by Eq. (32). The carrier mobility, in the absence of precursor-defect-related scattering, may be extracted from the vertical intercept of Figure 6. Our data give a value of $\mu = 960$ cm^2/V-s, quite reasonable given the doping of these devices, 4×10^{16} cm^{-3} [25].

Galloway et al. [26] and Sexton and Schwank [27] have reported a formally similar correlation between the mobility of *irradiated* devices and the radiation-induced interface-trap density, ΔN_{it}. Our results suggest that, prior to irradiation, the carrier mobility may contain information about precursor defects, which, upon irradiation, lead to interface trap charge.

5. Discussion

5.1 Motivating Picture

Both of the correlations discussed above suggest that defects present prior to irradiation are related to both the radiation-induced interface-trap and oxide-trap charge. Conceptually, it is useful to write the preirradiation channel resistance parameter of a given device as

$$\beta^{-1} \equiv \xi(t) = \xi_0 + \delta\xi(t). \tag{33}$$

Here, ξ_0 is the time-average of the channel resistance, determined primarily by phonon scattering and scattering from impurities at or near the Si/SiO_2 interface. The fluctuating portion, $\delta\xi(t)$, arises because changes in the occupancy of defects at or near the interface change the number of charge carriers in the channel at a given time, and also cause the defect-related scattering rates to vary with time.

Much data strongly suggests that the low-frequency excess (1/f) noise of MOS transistors (e.g., below 1 kHz) primarily reflects carrier-defect interactions with oxide traps that are more than a few monolayers from the interface [1,2,10,19]. (Of course, at significantly higher frequencies there is also information in $\delta\xi(t)$ that bears on defects at or much nearer the interface.) Therefore, prior to irradiation, there appears to be information in ξ_0 which may allow one to predict the postirradiation interface-trap charge and information in low-frequency components of $\delta\xi(t)$ which allows one to predict the postirradiation oxide-trap charge. Thus, the interaction of the current with defects present before irradiation may contain a significant amount of information that could enable one to predict the radiation response of MOS transistors via channel resistance and 1/f noise measurements, without the need for destructive testing of the device.

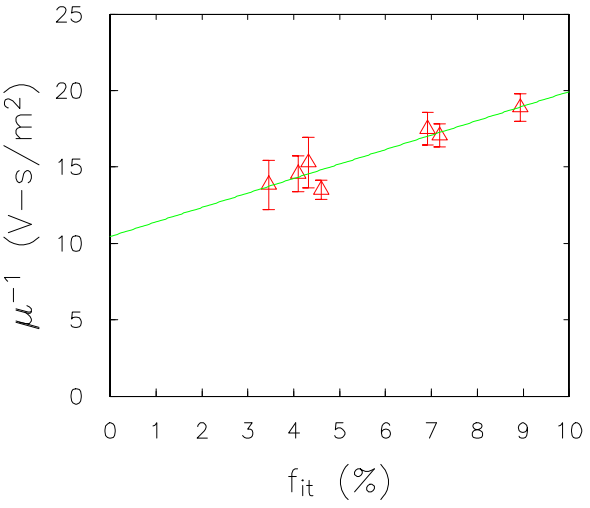

Figure 6. Preirradiation inverse channel mobility (μ^{-1}) versus interface-trapping efficiency (f_{it}). Values of f_{it} are derived from ΔV_{it}.

5.2 Implications for Hardness Assurance

It is generally quite difficult to draw conclusions about small (i.e., <20%) differences in channel resistances of arbitrary MOS transistors. There are a variety of reasons for this. First, the channel resistance depends upon the

[10] In fact, n_p and n_{pit} may be identical, i.e., $\lambda = 1$. Further work is required to determine whether n_p and n_{pit} are identical or simply proportional.

channel dimensions, and these are often not known with sufficient accuracy. Second, any differences in channel resistance must be viewed in the presence of a large phonon-scattering component common to all devices. Third, the measured resistance includes contact and series resistances which are specific to the device technology. Fourth, scattering from ionized impurities depends on the substrate doping. And, finally, various surface-scattering mechanisms are processing-dependent. As nearly all of these factors are the same for the seven G1916A wafers, we are able to draw conclusions from small differences in their channel resistance parameters. This would appear to be the case for most collections of nominally identical devices. Thus, it may be possible to use the preirradiation mobility of devices fabricated from a single technology as a predictor of radiation-induced interface trap charge. This correlation should be especially useful for long devices without lightly-doped drain extenders, so that variations in effective channel length and series resistance do not complicate the story. It is not likely that such measurements will be useful in predicting the relative radiation responses of devices fabricated with different technologies.

How useful might 1/f noise be in hardness assurance testing? Comparing the 1/f noise of various MOS transistors suffers from some of the same pitfalls as mentioned above in connection with channel resistances. Further, contact noise may completely mask noise originating in the channel. However, it is clear that noise measurements should be useful in determining the relative radiation hardness due to oxide trapped charge of devices fabricated with the same technology. Several factors suggest that noise measurements might be useful even for cross-technology comparisons. For one thing, there is not the large "offset" in the excess noise that there is in the carrier mobility (i.e., compare Eqs.(28) and (32)). This is reflected in the fact that the preirradiation noise levels vary by more than two orders of magnitude while the preirradiation mobilities vary by only about 30%. Thus, comparison of noise levels does not require accurate knowledge of the device dimensions. Secondly, one of the two cross-technology comparisons that we have made does agree with the scaling of Eq.(28). As mentioned above, the wafer that does not agree with the prediction may suffer from problems with its contacts and/or electron traps compensating hole traps [9]. We believe that the jury is still out on the usefulness of noise in making cross-technology comparisons -- clearly further work is needed.

6. Conclusions

We have found that the 1/f noise and channel resistance of unirradiated nMOS transistors from a single lot with various gate-oxide splits closely correlate with the oxide-trap and interface trap charge respectively following irradiation. The 1/f noise is explained by a trapping model, while the variations in channel resistance are explained by scattering from interface-trap precursor defects. It appears that both noise and channel mobility measurements may be useful in defining nondestructive hardness assurance test methods for devices fabricated from a single technology. It may be difficult to use either for making cross-technology comparisons. Finally, during the course of this study it was found that process techniques that improve the radiation hardness of MOS devices at room temperature can greatly reduce the 1/f noise of MOS devices at cryogenic temperatures.

7. Acknowledgments

The authors would like to thank Pete Klimecky, Matt Trawick, and Nick Borland for their assistance in noise measurements, and P. S. Winokur, P. J. McWhorter, S. L. Miller, and M. R. Shaneyfelt for stimulating discussions.

8. References

[1] John H. Scofield, T. P. Doerr, and D. M. Fleetwood, "Correlation between preirradiation 1/f noise and postirradiation oxide-trapped charge in MOS transistors," *IEEE Trans. Nucl. Sci.* **NS-36**, 1946-52 (1989).

[2] D. M. Fleetwood and John H. Scofield, "Evidence that similar point defects cause 1/f noise and radiation-induced-hole trapping in metal-oxide-semiconductor transistors," *Phys. Rev. Lett.* **64**, 579-82 (1990).

[3] John H. Scofield, M. Trawick, P. Klimecky, and D. M. Fleetwood, "Correlation between preirradiation channel mobility and radiation-induced interface-trap charge in metal-oxide-semiconductor transistors," *Appl. Phys. Lett.* **58**, 2782-4 (1991).

[4] K. H. Lee, John C. Desko, Ross A. Kohler, Cris W. Lawrence, William J. Nagy, Julie A. Shimer, and Steven D. Steenwyk, "Radiation hard 1.0 μm CMOS technology," *IEEE Trans. Nucl. Sci.* **NS-34**, 1460-3 (1987).

[5] P. S. Winokur, E. B. Errett, D. M. Fleetwood, P. V. Dressendorfer, and D. C. Turpin, "Optimizing and controlling the radiation hardness of a Si gate CMOS process," *IEEE Trans. Nucl. Sci.* **NS-32**, 3954-61 (1985).

[6] See, for instance, S.M. Sze, *Physics of Semiconductor Devices, 2nd edition.* (John Wiley & Sons, New York, 1981), p. 441.

[7] P. S. Winokur, J. R. Schwank, P. J. McWhorter, P. V. Dressendorfer, and D. C. Turpin, "Correlating the radiation response of MOS capacitors and transistors," *IEEE Trans. Nucl. Sci.* **NS-31**, 1453-60 (1984).

[8] J. J. Simonne, G. Blasquez, and G. Barbottin, "1/f noise in MOSFETs," in *Instabilities in Silicon*

Devices: Silicon Passivation and Related Instabilities, Vol. 2, (Elsevier, Amsterdam, 1989), pp.639-57.

[9] D. M. Fleetwood, R. A. Reber, Jr., and P. S. Winokur, "Effect of bias on TSC in irradiated MOS devices," *IEEE Trans. Nucl. Sci.* **NS-38**, No. 6 (1991).

[10] T. L. Meisenheimer and D. M. Fleetwood, "Effect of radiation-induced charge on 1/f noise in MOS devices," *IEEE Trans. Nucl. Sci.* **NS-37**, 1696-1702 (1990).

[11] S. Christensson, I. Lundstrom, and C. Svensson, "Low frequency noise in MOS transistors," *Solid-State Electronics* **11**, 797-812 (1968).

[12] F. Berz, "Theory of low frequency noise in Si MOSTs," *Solid-State Electronics* **13**, 631-47 (1970).

[13] S. T. Hsu, "Surface state related 1/f noise in MOS transistors," *Solid-State Electronics* **13**, 1451-9 (1970).

[14] A. van der Ziel, "Flicker noise in electronic devices," in *Advances in Electronics and Electron Physics, Vol. 49,* edited by Martin and Martin (Academic Press, New York, 1979), pp. 225-297.

[15] G. Blasquez and A. Boukabache, "Origins of 1/f noise in MOS transistors," in *Noise in Physical Systems and 1/f Noise,* edited by H. Savelli, G. Lecoy, and J. P. Nougier (Elsevier, Amsterdam, 1983), pp.303-6.

[16] Zeynep Celik and Thomas Y. Hsiang, "Study of 1/f noise in n-MOSFETs: linear regime," *IEEE Trans. Electron. Dev.* **ED-32**, 2797-801 (1985).

[17] O. Jantsch and B. Borchert, "Determination of interface state density especially at the band edges by noise measurements on MOSFETs," *Solid-State Electronics* **30**, 1013-15 (1987).

[18] Kwok K. Hung, Ping K. Ko, Chenming Hu, and Yiu C. Cheng, "A unified model for the flicker noise in metal-oxide-semiconductor-field-effect transistors," *IEEE Trans. Electron. Dev.* **ED-37**, 654-65 (1990).

[19] M. J. Kirton and M. J. Uren, "Noise in solid-state microstructures: a new perspective on individual defects, interface states, and low-frequency (1/f) noise," *Adv. in Phys.***38**, 367-468 (1989).

[20] J. H. Scofield and D. M. Fleetwood, unpublished.

[21] A. L. McWhorter, "Surface state related 1/f noise in MOS transistors," in *Semiconductor Surface Physics.* (University of Pennsylvania Press, Philadelphia, 1957), p.207.

[22] R. Jayaraman and C. G. Sodini, "1/f noise interpretation of the effect of gate oxide nitridation and reoxidation on dielectric traps,"*IEEE Trans. Electron. Dev.* **ED-37**, 305-9 (1990).

[23] R. Reif, *Fundamentals of Statistical and Thermal Physics.* (McGraw-Hill, New York, 1965), p. 351.

[24] P. Dutta and P. M. Horn, "Low-frequency fluctuations in solids: 1/f noise," *Rev. Mod. Phys.* **53**, 497 (1981).

[25] S. M. Sze, *Physics of Semiconductor Devices, 2nd edition.* (John Wiley & Sons, New York, 1981), p.29.

[26] K. F. Galloway, M. Gaitan, and T. J. Russell, "A simple model for separating interface and oxide charge effects in MOS device characteristics," *IEEE Trans. Nucl. Sci.* **NS-31**, 1497-1501 (1984).

[27] F. W. Sexton and J. R. Schwank, "Correlation of radiation effects in transistors and integrated circuits," *IEEE Trans. Nucl. Sci.* **NS-32**, 3975-81 (1985).